NATIONAL TECHNICAL UNIVERSITY OF ATHENS

Monotonic and Cyclic performance of Base-Plate Modelling on Non-Linear Finite Element Analysis and Computer Aided Engineering

THESIS IN CIVIL ENGINEERING

Master of Science in Civil Engineering

Thesis submitted to the National Technical University of Athens as a fulfilment of the requirements for the degree of

MASTER OF SCIENCE IN ENGINEERING

By Diogenes Marcel Ferreira Honda

February 24th 2022

Athens, Greece

By Diogenes Marcel Ferreira Honda

Monotonic and Cyclic performance of Base-Plate on Non- Linear Finite Element Analysis and Computer Aided Engineering Modeling

Diogenes Marcel Ferreira Honda, Candidate for the Master of Science Degree
National Technical University of Athens

Supervisors:
Ioannis Vayas, Structural Department, School of Civil Engineering, National Technical University of Athens
Bonaventura Taglafierro, University of Salerno

Abstract

Base Plates are accustomed to link member with their particular foundations. They're consistently found in cantilevered structures, traffic indicators, digital cameras and manufacturing warehouses and garages, these poles usually are supported on concrete footings. Consequently, the goal regarding this study will be create a process to model a base plate subjected to a tension pushover on its orthogonal axis inducing a tension on its plates. To perform the reported goal, a steel gauge is tested and a full-scale base plate is tested in laboratory underneath the uniaxial loading.

This thesis also involves the analyses of the fracture under the monotonic and cyclic loading. This Study was motivated to explore the possible spread of stresses, which by, brings the fracture phenomena.

Acknowledgements

Firstly, I would like to thank my thesis supervisor Professor Ioannis Vayas for all knowledge taught during the steel structures course during the master program and for being open for any questions along this research.

Additionally, I would like to thank the P.h.d. candidate Bonaventura Taglafierro from the University of Salerno, whom had been always available for any nature and magnitude of my doubts.

At last, I extend my sincere thanks to all my colleagues whom supported and assisted me along these two years and my family, in special my father for the encouragement in all the ways continue my studies.

Author

Diogenes Marcel Ferreira Honda

TABLE OF CONTENTS

1.0 Introduction

1.1 Background

Composed by cold formed thin walled steel members, rack supported structures are implemented mostly in rack storage systems (Figure 1) among other functionalities. Those are also ideal for climate controlled ware-houses as well as fits as no other structure in a matter of settlement of its system and the costs between production and installation.

Figure 1: Warehouse with storage racks

As well as poles with base plates are utilized as light poles in relaxation areas, recreation areas, and arenas which are outside. These utility poles are supported on tangible footings by way of metallic base plates, where a great part of those application are installed with levelling nuts, allowing the final and fine adjustment of level and alignment at the top of the structure.

Those used on utility frameworks ends up on causing membrane layer, flexural, and shear stresses within the metallic plate, as a result of gravity (self-weight) and crossing loads (wind/earthquake). Before a bases are created, a part modulus, should be determined so that you can determine the stresses being flexing the bottom plate. Presently, there is absolutely no rational strategy on identifying the efficient thicknessess for the plate to be utilized. Many designers count on either on estimation or

practices which are traditional tend to be perhaps not rationally-based, or they normally use expensive/time eating processed techniques of evaluation.

The arrangement of structure is associated as having a heavy load capacity compared with the available conventional and commercial structures known. A huge number of qualities may be listed around any engineering study, however, the current urgency is situated in the lack of sufficient rules and specifications on designing wherein.

The thickness additionally to its slenderness brings us a concern when discussed about the beam upright connections and base plates, where those are famous by having a lower capacity on its non linear phase than on linear phase.

In practice, a thicker base plate is much more cost-effective than the usual thin base plate with extra stiffeners or any other reinforcements (DeWolf1990).

1.2 Objective

Ductile materials exhibit two types of fracture: “ductile shear fracture” and “ductile tensile fracture” (Björklund and Nilsson 2014). Either mode or a combination of both may take place in structural steel (Hooputra et al. 2004, Björklund et al. 2013). Here, this study aims to analyse how a ductility in a base plate for racks would influence on its performance and how to approximate the modelling to the tests made on laboratory.

The modelling is based in a finite element analyses and Computer-Aided Engineering software, where helped to understand better the performance obtained in a monotonic test and in a cyclic loading test. Whereby CAE, Abaqus 6.13 and IdeaStatica were used to perform the monotonic test and the cyclic test, as well as SAP 2000 were used to perform the pushover analysis used as a parameter to the cyclic loading.

Understand the behaviour of a steel plate being pulled on its orthogonal direction is also an point to be mentioned here ahead, furthermore the analysis on utilising different parameters for ductility, here represented computationally as displacement until its damage.

1.3 Problem Statement

Base plates settled when fixed to a column structures tend to be generally supported on concrete footings. The Base plates tend to be connected to the footings making use of anchor bolts. Even considering the footing is a concrete grouted highly resistant base, it cannot be considered that it is able to support the extenuating movements as well as its loads. Additionally to the susceptibility for buckling on slender members seen on rack structures rises the necessity on studying such an issue based in a computational and experimental tests.

1.4 Scope

The research covers the force necessity, but, exhaustion and fatigue were not inside the range with this research.

The variables which are essential in this study tend to be the nature of applied load, wide range of bolts, spacing between bolts, distance amongst the bolts and face of this line dimensions for the base plate such as the width.

1.5 Methodology

The methodology stands for

- Study of basic concepts of steel structures

- Essential preliminary tests

- Tensile Test

- Extraction of values

- Tests performed on base plates

- Importing data among realized tests

- Exporting Values to Computational Modelling

- Finite Element Application

- Application of Results

- Computational Aided Engineering Modeling

- Analysis and Comparisons of results

- Conclusions

2. Tensile Test

2.1 Main Features

The principal attributes of structural-steel include technical properties like its weldability. In past times designers had a tendency to concentrate just from the tensile properties (longitudinal yield tension and ultimate tensile strengh), with some interest compensated into the deformability as calculated because of the elongation at break of the stress specimen. Considering that the modulus of elasticity, E, is continual for several reasons which can be useful all grades of metallic, it is hardly ever already been an option aside from for serviceability dilemmas. Weldability had been wrongly believed is sufficient for several steels ignoring many other parameters. Ductility or deformability was similar on its importance to some, where considering that the design requirements has actually offered just limited, specific needs.

Whenever metal is curved, you should keep carefully its stress-strain curve in your mind. If tensile force is placed on a metallic club, it shall involve some elongation. In the event that force is little adequate, the proportion associated with the tension and stress will continue to be proportional. This is often present in the graph as being a range this is certainly right zero and limitation of proportionality. In the event that force is greater, the materials will experience deformation nevertheless the proportion strain and stress won't rely. This middle point is known as elastic limit. Ahead of the elastic limit, we see plastic deformation where it starts to yield.

2.2 Previous Studies

Franstisek et al. (2008) studied the behaviour of base plates in flexing plus the anchor bolts in stress. An analytical design analytical was derived to anticipate the opposition and rigidity of base plate and anchor bolts. They considered two instances, versatile bolts and stiff-plate in touch with the concrete base, as well as, the plate apart from the base. They proposed that the causes which prying forces are being observed

created only if base plates come in connection with the base foundation. Experimental designs had been examined into the laboratory, with various bolts sizes and base plates thicknesses. With slim base plates, hinged where plastic were made before failure, whereas within the base plate just two hinge points had been made before the anchor bolts eventually folded to collapse.

The rise in bolt pitch led to exceptionally deformations which can be high didn't have any impact on the character of failure.

2.3 Introduction to the Tensile Test

Tensile examination is probably the most basic and several widely technical used tests. By calculating the force necessary to stretch a specimen to its limit point, the test enables designers and quality supervisors to anticipate exactly how products and items will act inside their desired programs.

Numerous overall performance variables could be calculated by well executed tensile screening. The ensuing information — a bend of force vs. expansion — programs the tensile profile associated with the test to the position where specimen pauses. Along this profile, the tensile brings numerous sights, main included in this, the flexible limitation and power to split or failure point.

Tensile evaluation provides information from the stability and security of products, elements and items, assisting industries on their particular finished services, products fit-for-purpose and produced into the high quality on its greatest.

Programs of tensile evaluation within the construction business feature brings, material and tensile strength-testing of geotextiles and security assistance netting, relationship power examination of glues, mastics, sealants and bonds.

Material and tensile strength-testing of geotextiles and protection help netting
Commitment energy study of adhesives, mastics, sealants and bonds between rock and foam amounts

Also referred to as a stress test, the most fundamental and typical forms of technical evaluating, a tensile test applies tensile force to a product and steps the specimen's a reaction to the stresses. Using this method, tensile examinations determine just how powerful a product is and just how much it may elongate. Tensile examinations are generally performed on electromechanical and really simple to do, and are also completely standardised.

2.4 Compute Aided Engineering (CAE) Modeling

2.4.1 Introduction

CAE or Computer-Aided Engineering is just a term to describe the task which includes a whole engineering procedure, from design and virtual assessment with advanced analytical formulas into the planning of production. Computer-aided engineering is standard in any business that utilizes some kind of design computer software to build up services and products. CAE may be the alternative in not merely creating an item additionally giving support to the manufacturing procedure, since it enables to execute examinations and simulations for the product’s actual properties without requiring a physical model. More commonly utilized simulation evaluation types include Finite Element research, Computational Fluid Dynamics, Thermal research, Multibody Dynamics, and Optimizations into the framework of CAE.

2.4.2 Geometry and main features

In order to have a standard of quality and function, a tensile test was performed with a steel gauge of 267mm length, being constrained at 20.23mm on one of the edges as an encastre and at the other edge as an uniaxial displacement control along according to the ISO 6892-1, additionally having a mean thickness of 5.99mm, an 80mm and a 90mm width (Figure 2(a) and (b)).

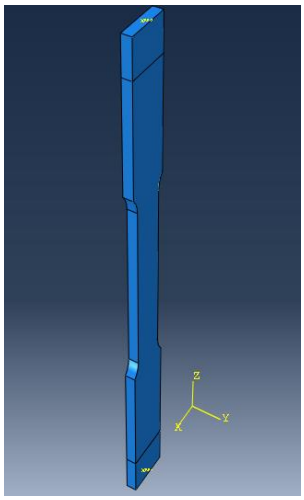

(a)

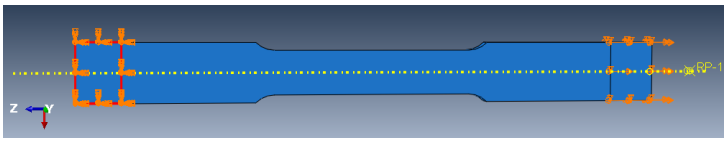

(b)

Figure 2: Main steel gauge geometry (b) and where encastre(left) and displacement (right) are positioned on the gauge.

2.4.3 Material Assumptions

The metallic specimen was characterized as a yield of fy=262.78Mpa, with a strain of 3.507% and an ultimate strain of fu=408.25Mpa on the strain of 47.988%.Those parameters defined by the stress x Strain curve were used to perform the same test on the CAE software.

As soon as the geometry is already defined, the next step is to define the properties of steel. The density(ρ) on “Material Design Properties for Structural Steel S235, S275, S355, S420, S450, S460 according to EN1993-1-1 §3.2.6” is approximately 7850 kg/m3. At the same table is also mentioned the Poisson's ratio in elastic range as ν=0.30 and Modulus of elasticity (Young's modulus) as E=210000MPa. The stress rate considered follows the criteria of the laboratory test as 0.9MPa/s.

2.4.4 Meshing

To be able to include the actual steel behaviour within the experimental examinations, different facets needed to be considered when making the Abaqus design. The essential data, Stress vs. Strain, is desired.

On conducting a sensitivity analysis to obtain a close to perfect mesh distribution, as well as, in addition to the global mesh size of 0.7, maximum deviation and minimum size control 0.1 pre- defined as 0.1mm, had the final 140868 elements (Figure 3).

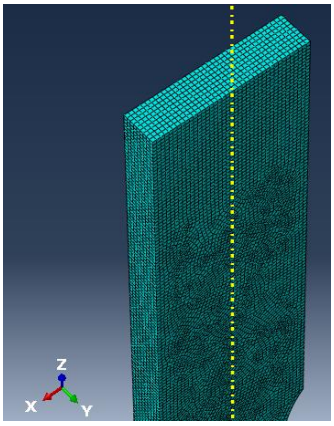

Figure 3: Mesh distribution where shows the lack of influence on meshing the displacement attach.

2.4.5 Stress Triaxiality

It is important to mention that stress triaxiality is one of the most common parameters to influence and reflect the stress rates. The behaviour and the relationship between stress triaxiality and fracture strain on ductile materials is also mentioned in the study of microstructural growth on McClintock, and Rice and Tracey.

The stress triaxiality can be defined as the product of the stress tensor and Mises stress (Equation 1(a)), furthermore the loading scenario to be considered on this case according to the criteria of failure of Von Mises is defined by the annulment of two

vectors here defined as x and y (Fig.3(b)). When everything is considered, the triaxiality is defined as 0.3.

$$\eta = \tau(\sigma`) \times 3(\sigma``)$$

(a)

$$(\sigma`) = (\sigma``) = (\sigma```) = 0$$

(b)

Equation 1: Definition of the stress triaxiality(a) followed by the assumptions to be taken on uniaxial tensile test pre-defined by Von Misses.

2.4.6 Fracture Energy (G)

The last two factors to be defined were fracture energy and displacement after fracture. Where, in order to define the damage required in terms of energy required for failure after the initiation of damage, the energy is proposed by Hillerborg in 1976, which follows the starin-stress curve after the ultimate stregth is reached in a form of area as a Mpa/mm2. Known as Hillerborg`s fracture Energy, is the energy required to trigger a unit area of crack this brings a clarity of how important it is, being defined also by the formula (Equation 2)

$$G_f = \int_{\varepsilon_0^{-pl}}^{\varepsilon_f^{-pl}} L\sigma_y \, d\varepsilon_f^{-pl} = \int_0^{u_f^{-pl}} \sigma_y \, du^{-pl}$$

Equation 2: Fracture Energy

Even considering that, the formula includes the equivalent plastic displacement and strain at failure and the characteristic length of the element, all of this can be simplified by obtaining the area in Mpa/mm2 after the plasticity has reached its limit regarding to

the stress-strain curve, multiplied by the characteristic length, shown and well demonstrated in the Figure 4.

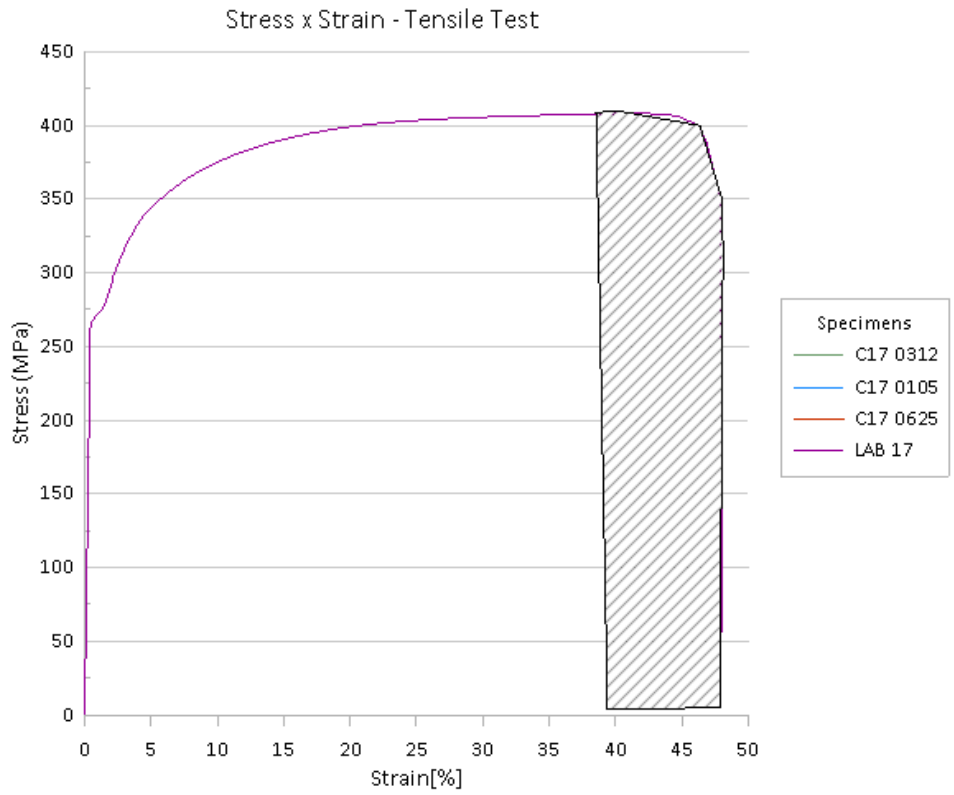

Figure 4: The Graph area considered to obtain the equivalent strain over the failure mode

Subsequently, two characteristic lengths must be considered since the fixed supported and the displaced area have different magnitudes, how ever, here is to be considered the total length instead the effective, once this has less than 1% of difference. Considering for the calculation the value of 38917.34mm3 as a volume and 6497.4mm2 as an area, resulting a characteristic length of 5.99mm.

Thereafter, adopting the area of 109.90MPa, the final product that also defines the fracture energy is given by Gf=27.19MPa .

2.4.7 Displacement at Fracture

Ductility is a vital function of the system, which makes it possible to deform inelastically without failure. The capability of steel made components to flex although not break is essential whenever afflicted by the effective and unexpected movements of earthquakes. A Few practices have already been recommended expressing the ductility of an assembly. One acknowledged dimension of ductility could be the proportion associated with top displacement to your yield displacement.

This meaning just views the structure's ability to produce until achieving its maximum load.

Although ductility is definitely an attribute that is essential, it must be mentioned that it's not really a material property and caution is utilized whenever researching different structural methods. Because of the variation that is out there whenever determining the rigidity this is certainly flexible yield load, a margin this is certainly big mistake and contradictory results exists.

Here, the displacement damage evolution has basically the same objective than the past one here mentioned but this time being summarized as the magnitude that measures how further the element tends to displace after the initiation of the deformation, therefore, categorizing the ductility feature.

After having a "neck" is continued to develop, the elongation, as being a measure of ductility, has got the drawback that it's truly consists of two components: the consistent elongation, occurring before necking, additionally the localized elongation occurring during necking. The component this is certainly 2nd responsive to the specimen final shape.

2.5 Tensile test results and comparison

Being defined as the double of the fracture energy divided by the ultimate strain, for this model it was calculated the value of 0.0312mm, taken as a reference and being also

compared with the behaviour among the displacement factors of 0.0105mm and 0.0625mm.

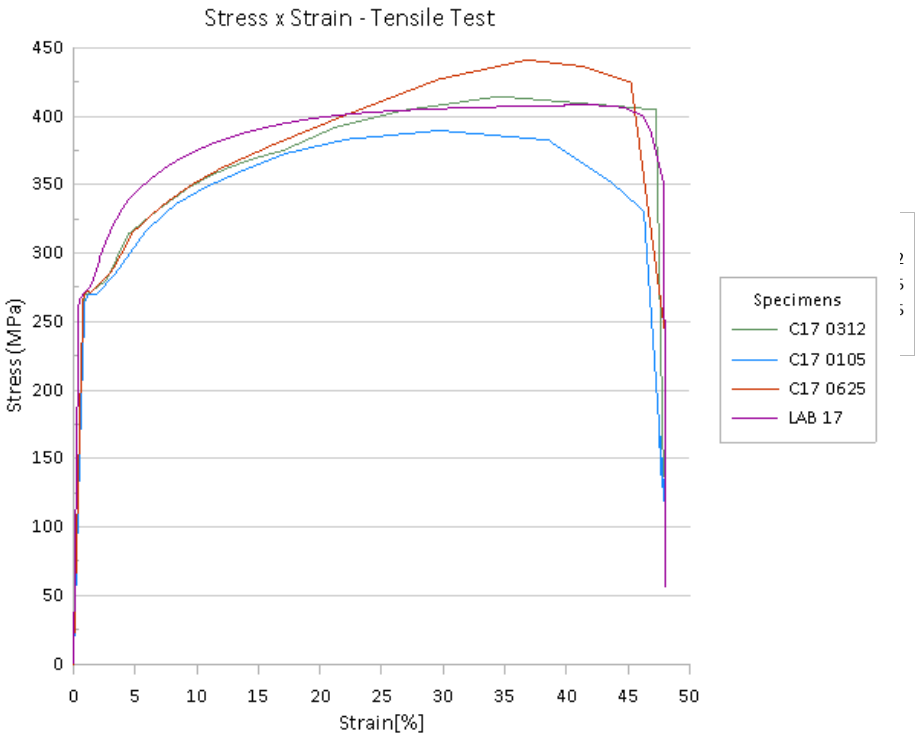

Figure 5: Strain x Stress Curves Comparison

It is observed at Figure 6, that the curve closer to the specimen tested in the lab is the expected one C17 0312, where for this on its name, the number represents the displacement after fractures previously mentioned. By conclusion it is also clear that as soon as the displacement is larger the element demands a greater magnitude in order to step out of the damage and reach the final area, here, being characterized by the higher curve, whereas, gaining an angle as soon as it reaches the plastic strain, named C17 0625.

The last but not the least, the C17 0105 presents an interesting shape, where the element is not allowed to extend when as the damage is initiated being way down all curves, but literally having the same shape.

The damage turns to be well demonstrated when compared, rupt failure and small displacement post damage. In the other hand, the C17 0625 presents many bristles (Figures 6 (a) and (b)).

At last, but not the least, it is essential to mention the initial difference of 10,8% to 12,8% in the stresses values, where it is explained by the fact this is not a virgin material.

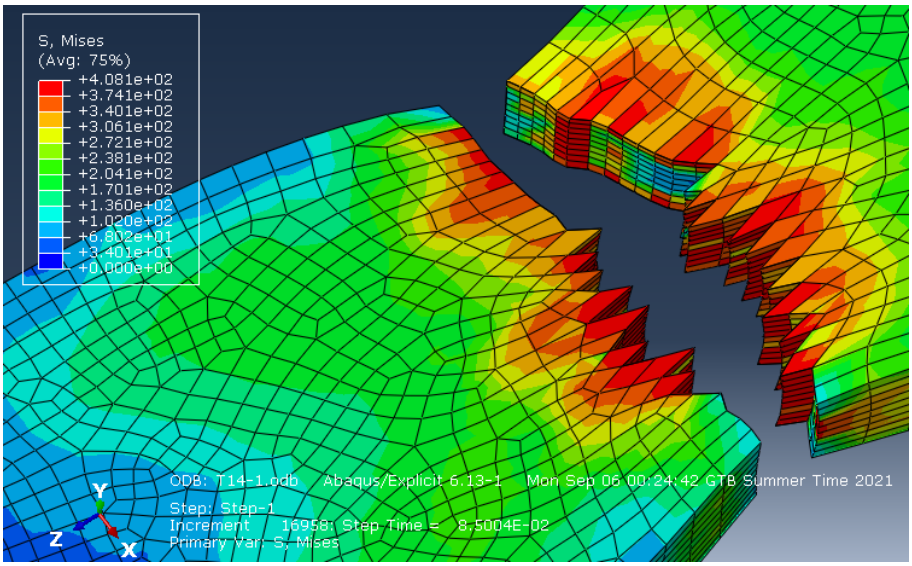

(a)

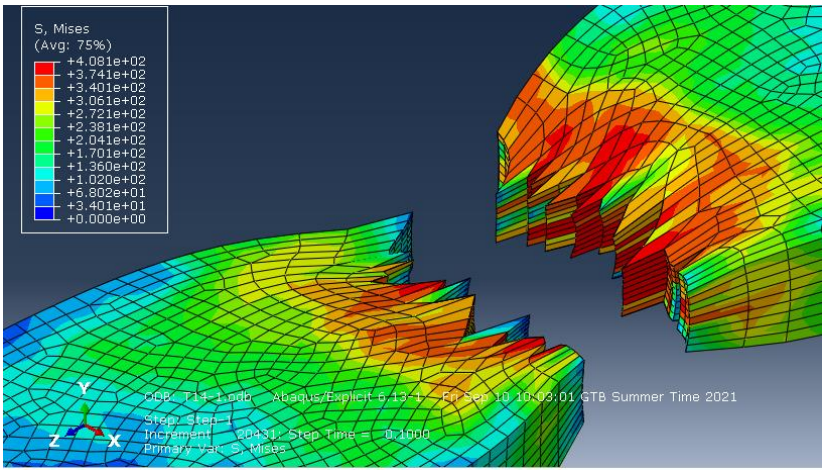

(b)

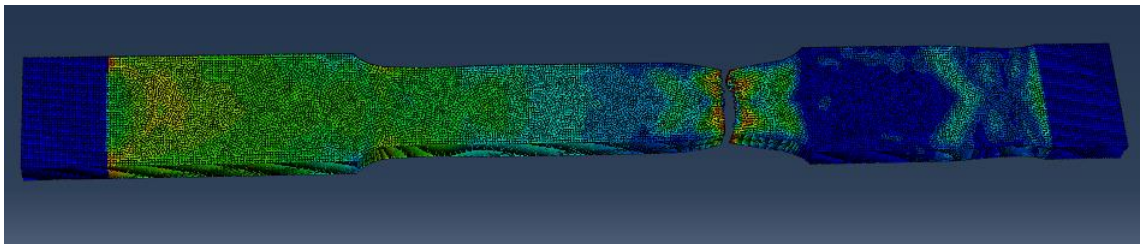

(c)

Figure 7: Deformed shape of C17 0105(a), C17 0625(b) and (c) C170312

3.Cyclic Test

3.1 Introduction

Base plates on rack structures are certainly crucial where created and designed to withstand the causes resultants in the base of the column. A rack's stability can also be prone when uplift causes the effect of a forklift collision or even to seismic causes brought on by a quake or wind causes, as well as the downward causes produced by the extra weight of this kept lots. Column base plates and anchors come together maintain the racking framework in an upright place, decreasing the chance of a failure and enhancing the security of workers employed in the location.

Once they truly are correctly attached to the column, base plates accept these concentrated loads and circulate all of them consistently over their bearing surface.

3.2 Main features

With 400mm long and 160mm large plate and a neck base with 123mm, 76mm and 184mm high, a base plate with 5mm was chosen to be tested over a cyclic load as shown on the figure 8. Before adding here the details regarding to the cyclic parameters, it is important to mention that, adaptations must be done even in the geometry. The base plate geometry was firstly settled and consequently tested, however, it is known that the

complexity might take the computing to a redundancy and a lack of quality in the results.

Firstly, one of the modifications undertaken was the addition of a “shadow” to simulate the contact between the bearing surface and head over the base plate hole, see Figure 9.

For the horizontally positioned ones there was no need to perform such an adaptation since only the shank influence the stress to be applied. All stresses induced on bolts itself, at first, are ignored. Only and exclusively the base plate is analysed, this simplification saves time and quality on results. Furthermore, the whole base plate ended on being cut over the orthogonal direction due its symmetry as shown on figure 11.

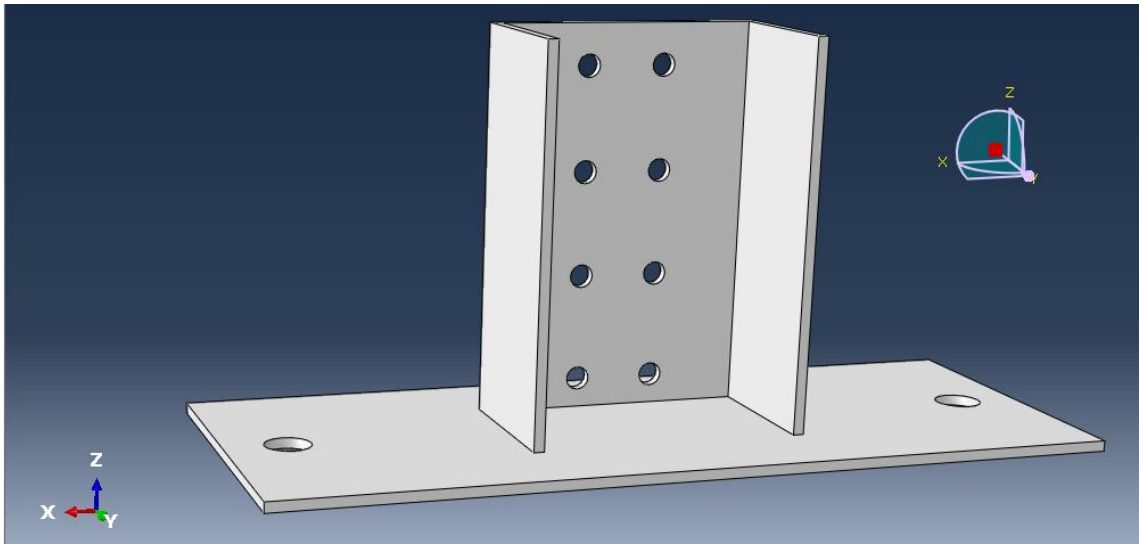

Figure 8: Base Plate

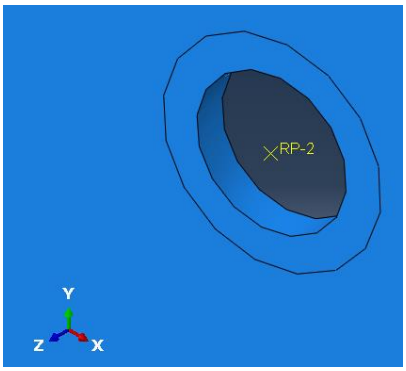

Figure 9: Bearing face being represented an encastre.

The material was defined and assigned to the base plate as the tensile test. Two reference points were created (Figure 12), one of them in the centroid of the neck void to measure the displacement upwards, and the other, over the bold void to verify the resistance force. A coupling interaction was assigned to the reference points to attach the face where it supposed to have an average of data. No other interaction was necessary.

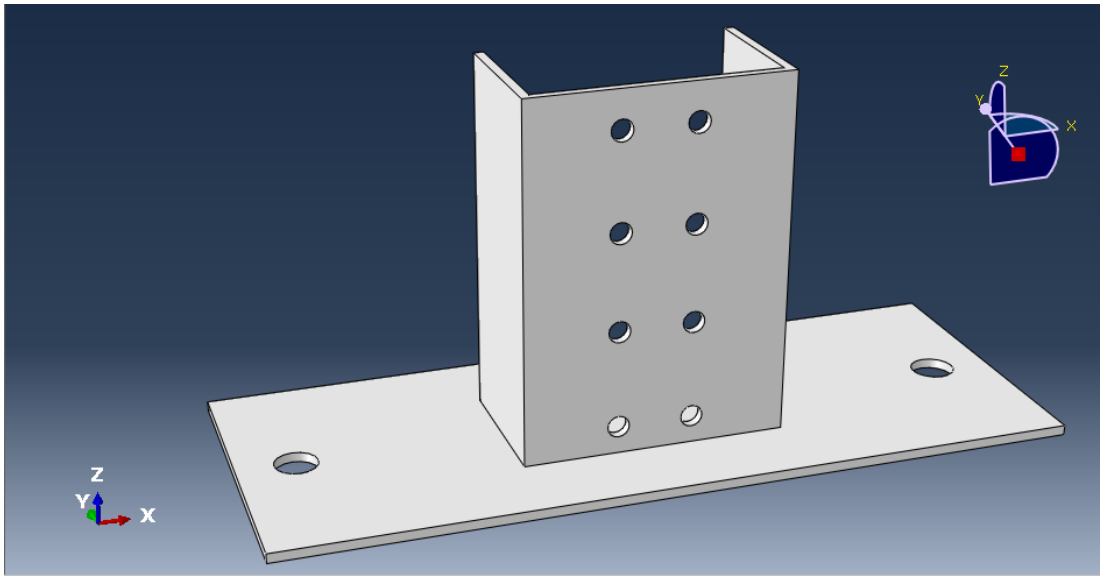

Figure 10: Perspective of base plate

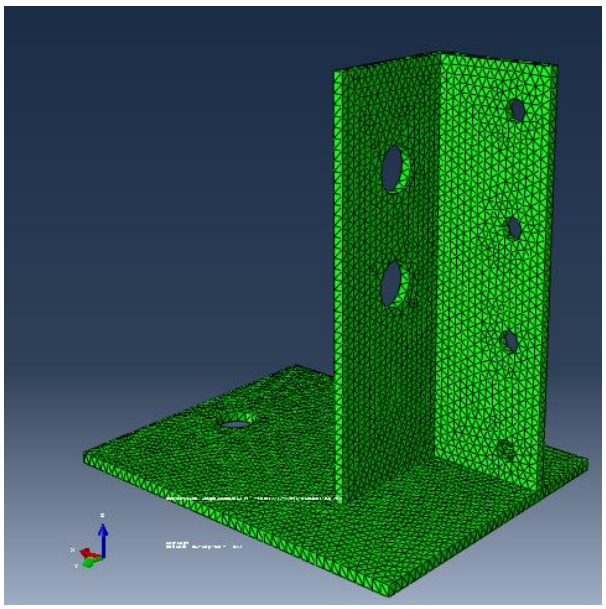

Figure 11: Perspective of the final geometry, cut in a half of “Y” axis

Still beside of everything mentioned above, a sensitivity analysis done on the model, it was possible to define the best and most refined meshing size 79170, based on the optimized global size of 2.995mm on seed control with a curvature factor of 0.12 and minimum size of 0.1mm, resulting on the distribution as shown in the figure 13.

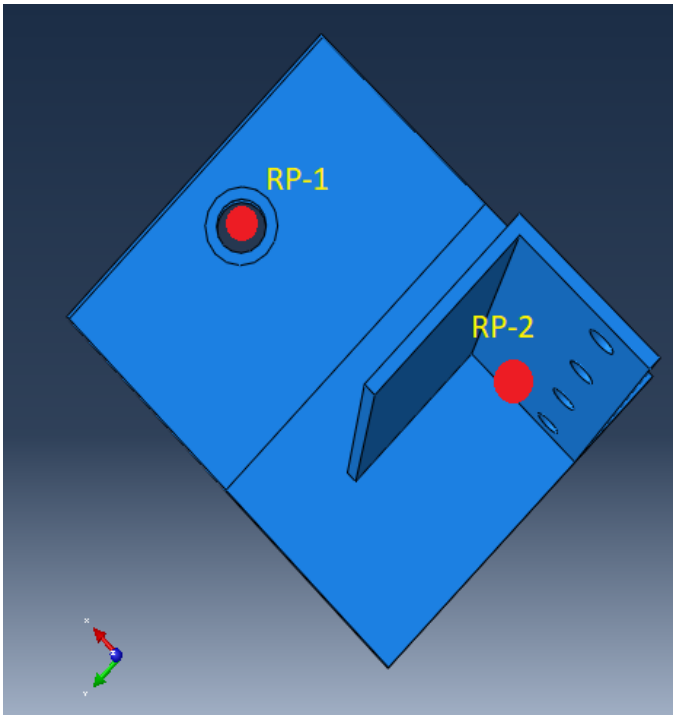

Figure 12: Top view with two reference points

Three boundary conditions were created preserving its individuality. The pull up might bring several different degrees of freedom, once tested, added the number of mesh elements, returned a poor result and more than 600.000 DOF`s. Therefore, the structure was limited on moving exclusively towards the “Z” axis and the rotation around the “Y” axis also allowed, knowing that once the plate when deformed rotate upwards to obey the system(Figure 14 and Figure 15).

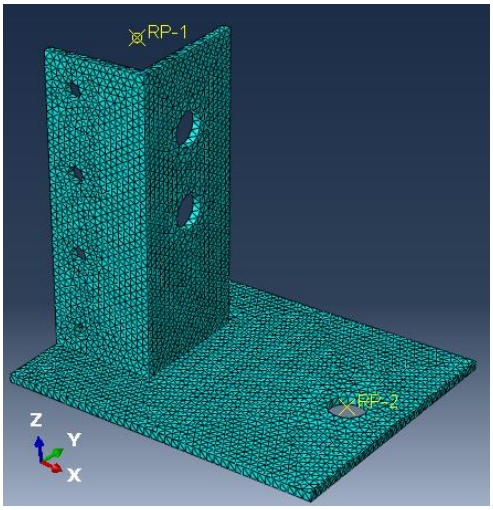

Figure 13: Mesh applied

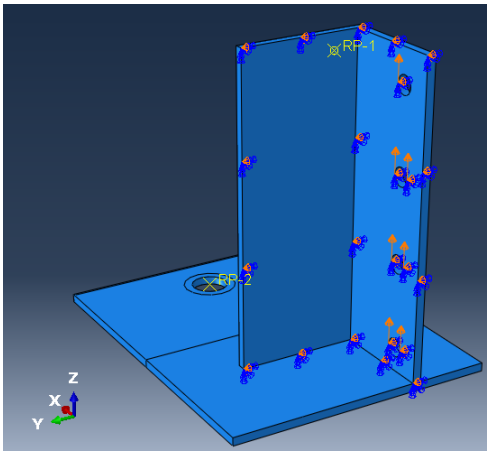

Figure 14: Perspective view demonstrating the disposition of the boundary conditions

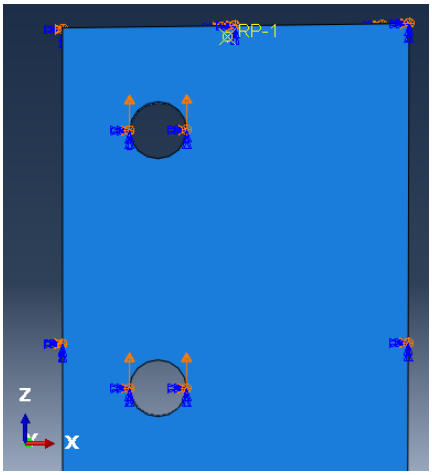

Figure 15: Front view illustrating the wholes where the base plate is pulled up

3.3 Previous Studies

Many researches in the past are suitable to be adapted in this study, main of the studies were revealed after Northridge (1994) Hyogo-ken Nanbu (1995) earthquakes steel frame base plates were characterized by their poor performance.

Among these studies the focus on finite element simulation became essential along the years (Kanvinde et al. 2013, Stamatopoulos and Ermopoulos 2011). One of the main references to this study is the study produced by James Swanson and Roberto Leon, where was put to test a T stub shaped connection in interaction to its components. In this same study, it is mentioned the T-sutb Connection Stiffness Model, the tension distribution along the plate, bolt stiffness as well as points treated also here like deformation at fracture, bringing an approach to and slip mechanism.

3.4 Finite Element Analysis

3.4.1 Introduction

Finite Element Analysis (FEA) involves simulating the behaviour of the component or installation under offered conditions such in a way utilising the factor finite element method (FEM). FEA can be used by designers to simply help simulate phenomena being actual thus lessen the dependence on actual prototypes, while enabling the optimization of elements within the design means of a task.

FEA utilizes models which can be mathematically understood and quantify the results of real-world circumstances for a component or installation. These simulations, that are carried out via specialised software, enable designers to discover prospective problems within a design, including regions of stress and places with a poor feature.

3.4.1.1 Structure Layout

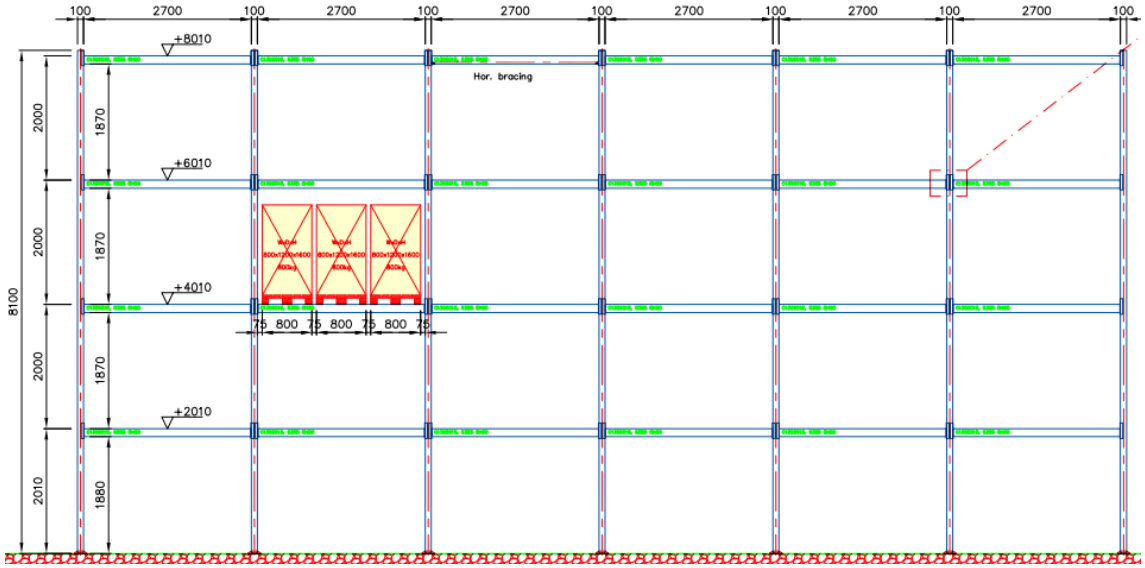

Figure 16: Full structure Front view

The structure defined to be studied has 8.1m tall and four slabs being divided by 2m height. By the longitudinal section the slots are divided by six spaces of 2.7m, and additionally to the column width of 100mm we have total 16.9m long (Figure 16).

The side view was taken for this study due its slenderness on its cross-section suffering from most of the deflection either on the service induced use or a ground motion. The side view has 1.1m long (Figure 17 (a)) being composed by trusses with different lengths of 1035.0mm, 1128.6mm, 1196.3mm and 1371.6mm.

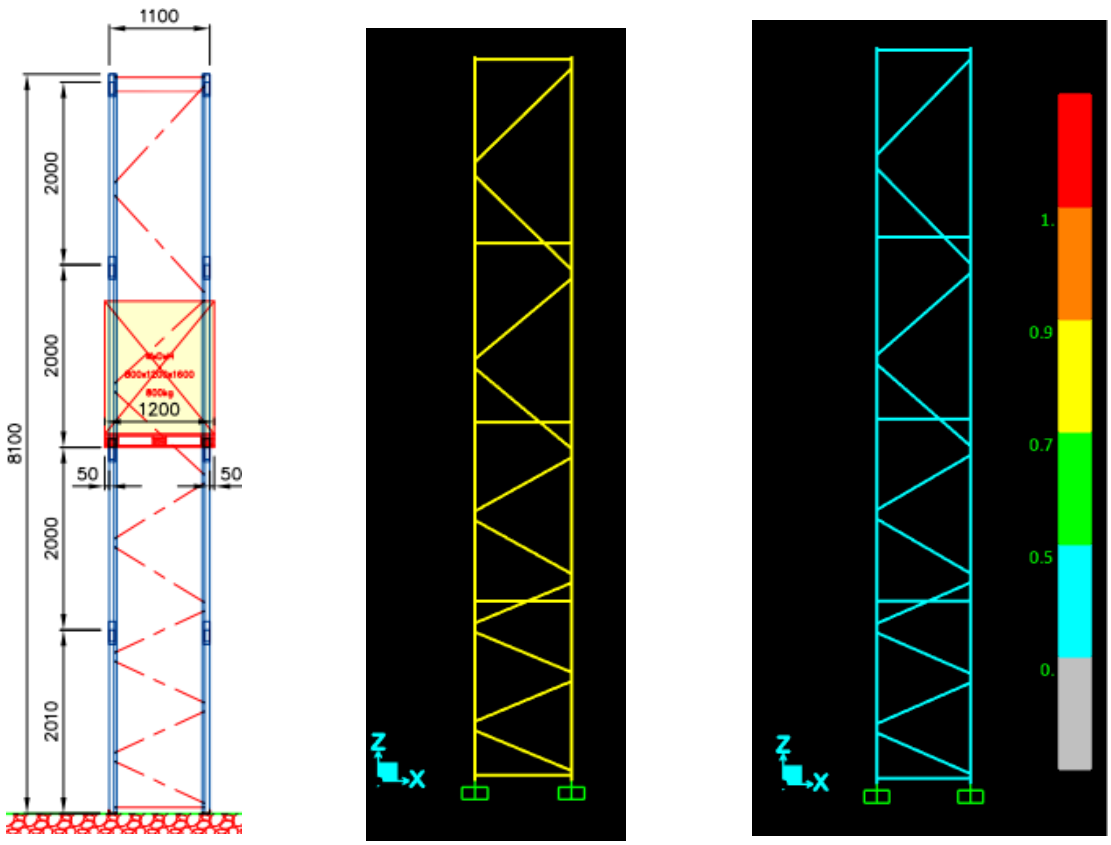

(a) (b) (c)

Figure 17: (a)Main side view layout [mm] (b) Layout Transferred to SAP 2000 (c)Design check on SAP 2000

3.4.2 Application

Since there is no regulation to determine where the base plate is fixed, it was adapted as a soil type C, the same utilized by the structure designer. The same determined the importance class II where this one brings the importance factor 1.0 .Based on the Eurocode 1998-1 and in the local Greek annex “ELOT EN 1998-1”, and adopting 475 years as a return period, the peak ground acceleration adopted is 0.25g. Having a cross sectional area of one column as 1160mm2 and one of the braces as 406mm2, we are able to get the stiffness as well as the masses (Table 1 and Table 2) to get to a final natural period of 0.1s.

Reference	Type	Cross Area mm2	Length mm	Young`s Modulus N/mm2	Stiffness N.mm
1	Columns	1160	8150.0	210000	29889.57
2	Columns	1160	8150.0	210001	29889.71
1	Braces	406	1035.0	210002	82377.60
2	Braces	406	1128.6	210003	75546.38
3	Braces	406	1128.6	210004	75546.74
4	Braces	406	8150.0	210005	10461.60
5	Braces	406	1128.6	210006	75547.46
6	Braces	406	1196.3	210007	71269.85
7	Braces	406	1196.3	210008	71270.19
8	Braces	406	1371.6	210009	62164.66
9	Braces	406	1371.6	210010	62164.96
10	Braces	406	1371.6	210011	62165.25
11	Braces	406	1371.6	210012	62165.55
12	Braces	406	1035.0	210013	82381.91
Total Stiffness					852841.43

Table 1 – Description of members Stiffness and Total Stiffness

Reference	Type	Cross Area mm2	Length mm	Volume mm3	Density kg/mm3	Mass kg
1	Columns	1160	8150.00	9454000.00	7.90E-06	74.69
2	Columns	1160	8150.00	9454000.00	7.90E-06	74.69
1	Braces	406	1035.00	420210.00	7.90E-06	3.32
2	Braces	406	1128.59	458209.29	7.90E-06	3.62
3	Braces	406	1128.59	458209.29	7.90E-06	3.62
4	Braces	406	8150.00	3308900.00	7.90E-06	26.14
5	Braces	406	1128.59	458209.29	7.90E-06	3.62
6	Braces	406	1196.34	485713.31	7.90E-06	3.84
7	Braces	406	1196.34	485713.31	7.90E-06	3.84
8	Braces	406	1371.58	556860.51	7.90E-06	4.40
9	Braces	406	1371.58	556860.51	7.90E-06	4.40
10	Braces	406	1371.58	556860.51	7.90E-06	4.40
11	Braces	406	1371.58	556860.51	7.90E-06	4.40
12	Braces	406	1035.00	420210.00	7.90E-06	3.32
Total Mass						218.28

Table 2 – Description of members Masses and Total Mass

The equations found in EN 1998-1/3.2.2.2 the elastic response spectrum was set for 5% damping and as type 1 (Figure 18). Since the importance factor corresponds to 1.0 the peak ground acceleration remains the same than the reference peak ground

acceleration(EN 1998-1/4.2.5(5)P). The parameters recommended for ground type C, it is also input the soil factor S =1.2, lower limit of period of constant spectral acceleration branch, TB 0.15s, upper limit of period of constant spectral acceleration branch TC=0.5s, beginning of the constant displacement response range TD=2s.

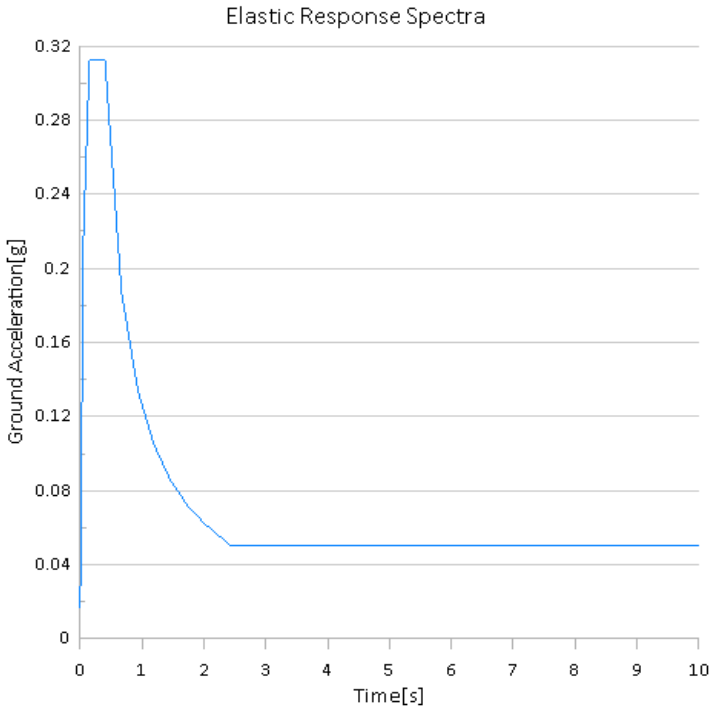

Figure 18: Elastic Response Spectra

3.4.3 Behavioural factor

Either for planar or spatial structural model, the required method of analysis and the behavioural (EN 1998-1/6.3.2) factor are influenced by the regularity of the structure. Here, q=4,0 will be adopted as mentioned in the EN 1998-1 Table 2 "c) Frame with eccentric bracings".

The combination of loads here is basically considered as a dead load and imposed load, where for the imposed load, following the FEM "Recommendations For The Design of Static Steel Pallet Racks in Seismic Conditions".

As in Abaqus, the material is defined with the same properties, as well as even the shape was defined as the geometry. A response spectrum curve was defined as the standard cited on European norms. Then, in the load cases, self load is taken into consideration, as a zero initial condition and to be considered as a non linear load. Afterwards, it is also created a non linear pushover load assuming the acceleration given on the spectrum curve. In an analysis of the worst case scenario, only two load combinations were necessary.

The frame arrangement is composed by 4 slabs being laterally embraced varying from 450mm until 1050mm, additionally to the 1100mm column spam (Figure 16). This braces are also included on the definitions on SAP 2000. Where the hinges are found, columns were set allowing the moment M3, and braces separated to receive entirely axial stresses. The Load combination set was a combination of dead load, maximum load from pallets and earthquake load:

SEISMIC UPLIFT – DL + PL + EL = 30kN

Restricting the structure to perform on “X” and “Z”, the analysis in done and the pushover curve is gotten. The base shear here, comes slightly under the 240 kN (Figure19). Another important data to be considered are the displacement and rotation obtained on the top of the structure. On the nodes 2 and 18 were found the magnitude of respectively 220.20 and 162.15 degrees. Deformed shaped due the lateral load on axis “X” is shown on Figure 20(c). It is also important to mention that the failure at the structure reflects the stresses observed on Figure 18.

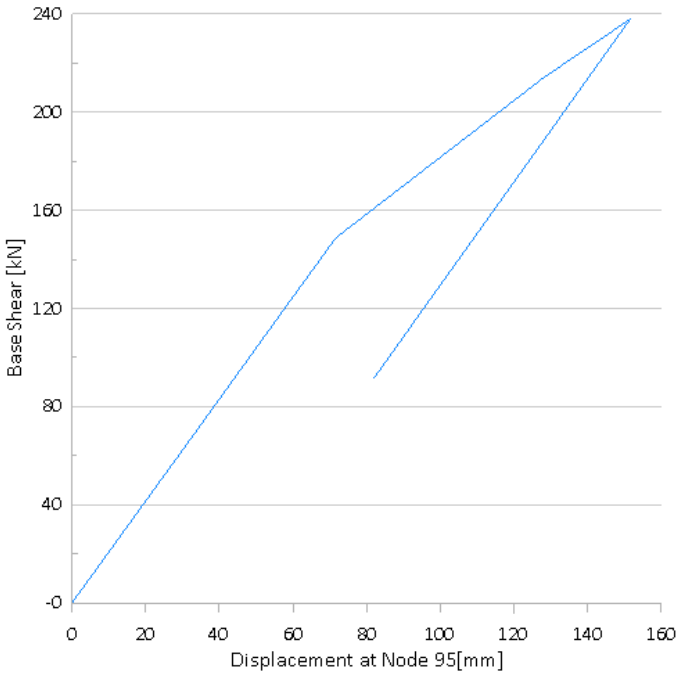

Figure 19: Displacement on node 95 [mm] x Base Shear [kN]

The failure mode is ended on this study in six steps, where the failures develop from the braces level by level. Where this last one fails first than the beams and columns yielding or buckling as shown in the Figures 20 (a), (b) and (c).

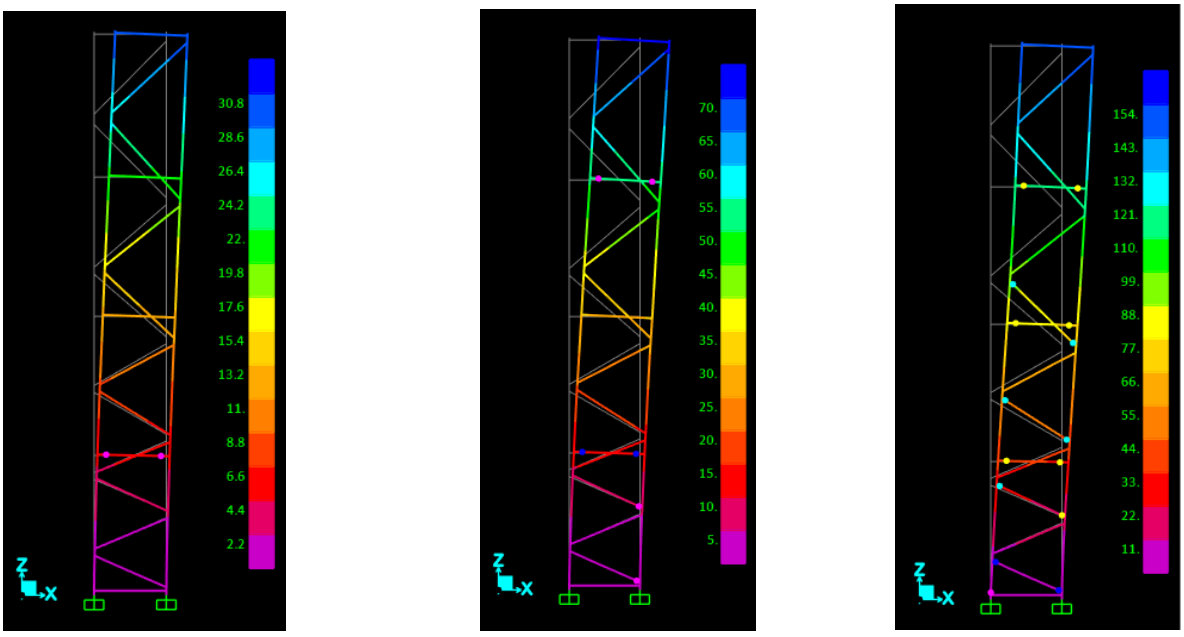

(a) (b) (c).

Figures 20: (a), (b) and (c) development of failure mode.

3.5 Cyclic Loading

These cyclic excitations is of such magnitude force connections tending to be obligated to act inelastically. Some experimental work with the consequence of cyclic loadings in the behaviour of big structural-steel cantilevers and their particular connections is explained, and also the answers are examined in this paper. One of many evaluations which can be essential in the analysis is between all-welded beam-to-column connections and connections with welded flanges and bolted plates.

3.5.1 Amplitude

Since the test is made based in a displacement control, a boundary condition was created as a displacement being ruled by an amplitude based on AISC Seismic Provisions (AISC 2002). To apply such rule, it was necessary to simulate and test the whole structure. This time SAP 2000 was the software necessary to obtain certain data.

Sequentially, according to the AISC Seismic Provisions (AISC 2002), the qualifying cyclic tests for beam to column shall be conducted by the story drift angle, as:

(a) 6 cycles at $\theta = 0.00375$ rad
(b) 6 cycles at $\theta = 0.005$ rad
(c) 6 cycles at $\theta = 0.0075$ rad
(d) 4 cycles at $\theta = 0.01$ rad
(e) 2 cycles at $\theta = 0.015$ rad
(f) 2 cycles at $\theta = 0.02$ rad
(g) 2 cycles at $\theta = 0.03$ rad
(h) 2 cycles at $\theta = 0.04$ rad

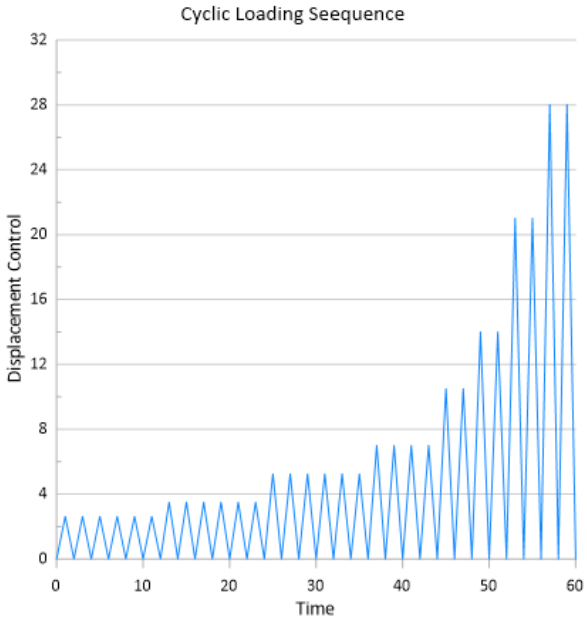

Figure 21: First Time Displacement distribution

However, the detailing of the amplitude to be followed is not enough to define the final results to be compared to the real velocity set in the laboratory at 0.15 mm/s.

3.6 Detailing the results on increments per step

This sequence resultant, after defined all rotations, is plotted at the amplitude, therefore for each displacement path is done is considered a step to be followed, then initially 60 steps to complete de cycle of 28mm. Those steps, as long as the results are ran, demand to be broken in to small pieces to satisfy Jacobian for numerical integration with the Newton-Raphson scheme, where Jacobian at the Gauss points are used for mesh verification. By definition, this mentioned, maps the parametric element to the geometric element. Those steps can still be optimized, calculating the stable size increment, where it can proceed to solve as a wave propagation problem.

Here, all users face a big problem, where by standard Abaqus tends to a simple element in a matter of 12 hours. Of course it is easy to define a time step as 1s, so for this case it would take 60s to finish, however the stability of the element might be compromised leading to a wrong failure mode since a stable time increment depends bases itself on density, stiffness and size.

Using the linear elastic properties on Young`s Modulus 210000MPa and with poison ratio (ρ) as 0.33, we are able to obtain the dilatational speed cd=797.72, based on Meyer at Equation 3(1):

$$cd = \sqrt{\frac{E}{\rho}}$$

Equation 3 (1)

I addition to the characteristic length Lc= 5.99mm, the stable time increment (Δt) results in 0.0000075089 expressed on the Equation 3 (2):

$$\Delta t = \frac{L_e}{C_d}$$

Equation 3 (2)

Another way can also be applied to equalize the reality with the simulation, here also tested. Once the test were done in a 0.15mm/s on the specimen, the displacement can also be divided resulting in 2799.2s long, this time not adapting the the analysis and but yes making it run in the real time basis, shown at the Figure 22.

This final distribution must has two references, where one of them if given by the software itself requesting not a precise stable time increment but at least where should it start from.

After the analysing mesh quality ABAQUS recommends a stable time increment less than 0.0001s, in the other hand, if we consider the mass scale basis(Equation 4) it returns 5.535x10^-5s.

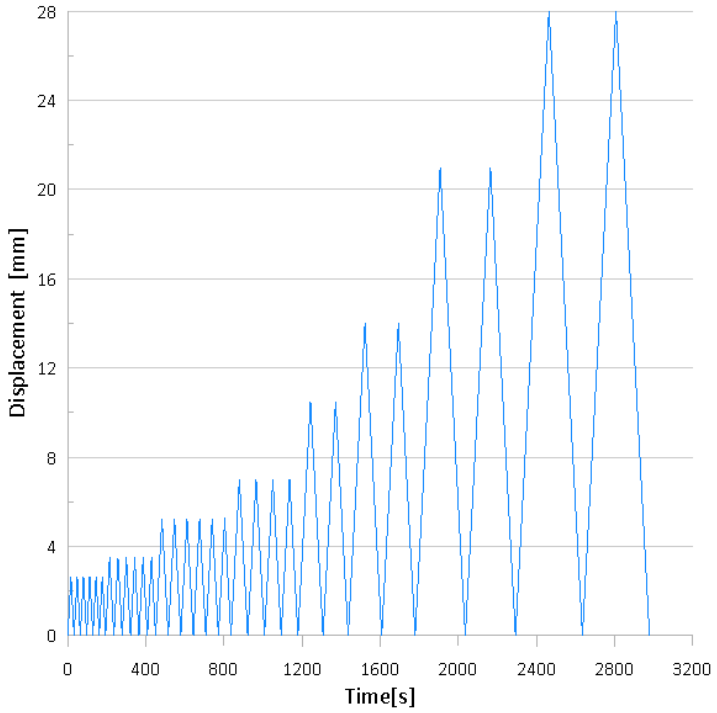

Figure 22: Time Displacement amplitude adapted to the real testing time

$$\Delta t = \sqrt[3]{\mathrm{V}} \times \sqrt{\frac{\mu}{\mathbb{E}}}$$

Equation 4: Stable time increment based in the mass scale

Summarizing the info above, the increment detailing is separated in three on ABAQUS, where by the minimum can be calculated in order to salve time on the usage of maximum eigenvalues and fraction critical dumping, however in the end, when necessary the software will reduce the increment by itself, it is extremely important to define the minimum possible, considering that, the minimum must just be analysed according to the outgoing of the whole submission analysis, repeated values and multiple attempts of solving the same step, will result in auto abortion.

Beside of the minimum, the last and least important, the definition of the maximum value might be used to define as accurate your model will discretise the result. In order to obtain a standardize the steps, the maximum increment per step will be the same than the minimum calculated, this way on running the analysis it wont be induced to the skip data, which might cause an abrupt and random element failure, forcing the analysis to

auto stop. It will increase the file sizing as well as the time to a full process however it will lead to a detailed enough for any other usage of data.

On comparing the results among the cyclic results, it is possible to find a few key points, represented by the red circles, showing a jump on the abrupt application of compression to force the specimen to return to its original position:

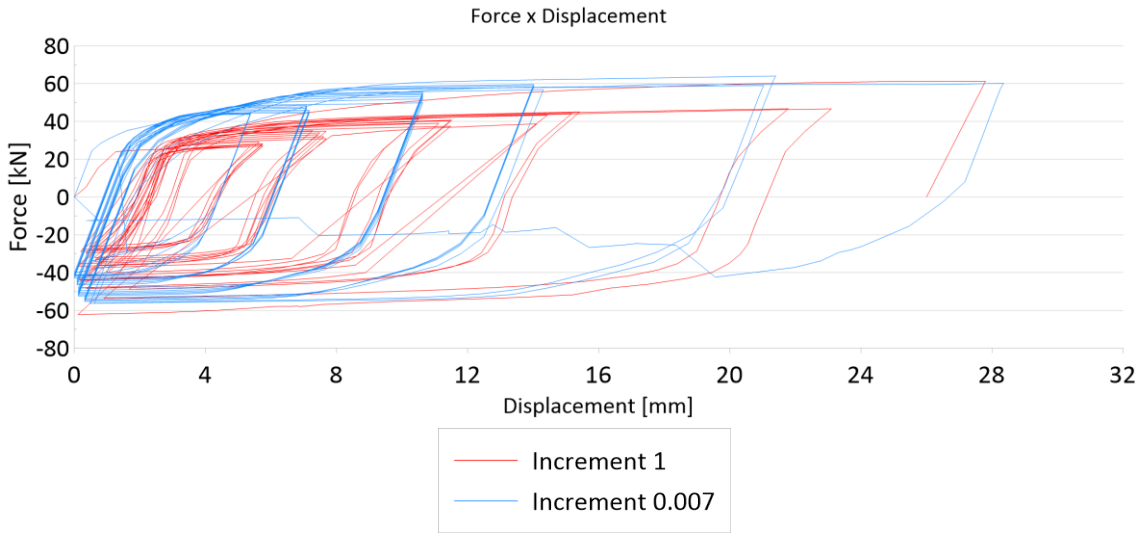

Figure (23): Displacement Force Graph, where the lack of physics parameters enough brings a wrong compression development

The graph demonstrates a good behaviour whereby matches with the strains stress curve and the monotonic test. At this point the model obeys a symmetry where ignores the real physics during all compression phases (Figure (23)) when compared with the laboratory results.

It ends up becoming mandatory the input of base plate bolts as well as the slab, where this last one is set as a rigid body undeformed and bolts M20 made of 8.8 class high strength steel.

3.7 Slip Behaviour

Eurocode 3 refers to a slip resistance of a pre loaded class 8.8 bolt should be taken as (Equation 5):

$$F_{s,Rd} = \frac{k_s \times n \times \mu}{\gamma_{M3}} \times F_{p,C}$$

Equation 5: Slip resistance

Where ks, bolt type factor, is given by the “Table 3.6: Values of ks”. Here adopted as 0.7(Bolts in long slotted holes with axis of the slot perpendicular to the direction of load transfer.

The contact between the bolt thread and the slot hole, the main slab and the bottom face of the plate and the bearing surface and the upper surface, gathered, form six friction planes, defining as the `n`.

Slip factor is selected by the category of the connections, for this study it was selected the category A (slip resistant and bearing type) as preloaded bolt suffering a shear stress, resulting in the slip factor 0.5.

Where necessary the analysis on ultimate limit state, the category A, this one using the recommended value for slip factor . In the other hands, we necessary regarding to to the serviceability, the safety factor according to “Table 2.1: Partial safety factors for joints” the recommended value becomes 1.25 .

In accordance with the ultimate tensile load of 830N/mm2 and the nominal stress area of 303mm2 in the use of the equation, it is obtained the preloading force of 176,043kN. In the end the slip resistance to be input in the contact interaction of the bolt is 295.752kN.

Beside of the slip condition, it is also important to mention that contact interactions were defined as among all surfaces by kinematic constrains where the slip behaviour is set on the tangential directions.

3.8 Final Results

After inputting all parameters gotten from the validation of the material like Stress x Stain curve among others and the dynamic behaviour when the contact influence the deflection of the model, it becomes clear to see the difference on the compression mode, another characteristic is the shape of the monotonic test where covers all the past results not presenting any abrupt deviation greater than 7% on the force peak on tension and 5% on the compression phase.

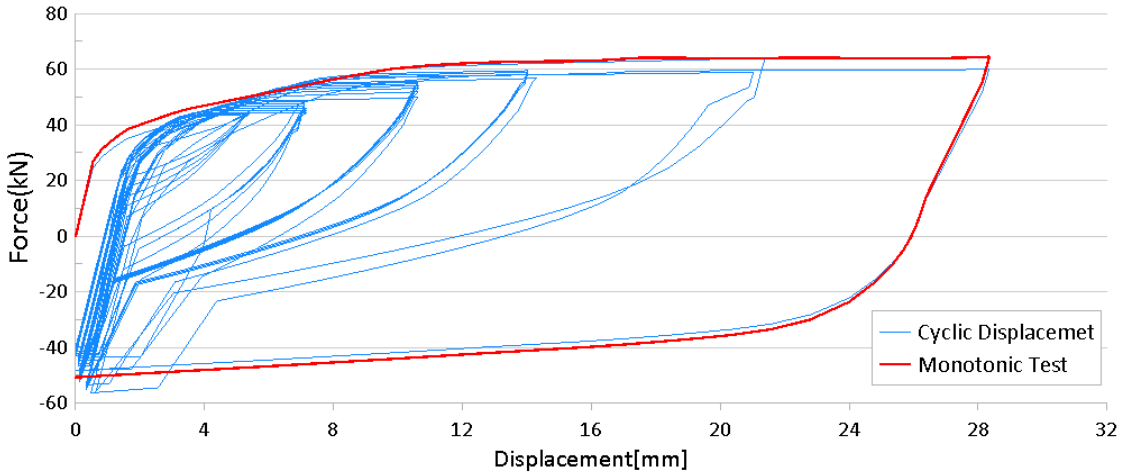

Figure 24: Force displacement with parameters corrected

The distribution and development of the stresses, here on the Figure 25 in a larger scale just for a representative matter, shows that as long as the displacement is imposed spots of the increasing of stresses rise around the bolt thread and on the side of the base where the columns is fixed.

This resultant behaviour of the amplitude proves the functionality of the first apparent over restrained boundary conditions on the column gap, voiding the structure to bend to dissipate an energy for a misplaced and undesired direction, this one increasing the complexity of the analysis, increasing the number of degrees of freedoms due to its irregularity comparing with the limitations imposed (Figure 26 (a), (b), (c) and (d)). The

symmetry function voids one of the continuances of the flange to buckle towards X axis.

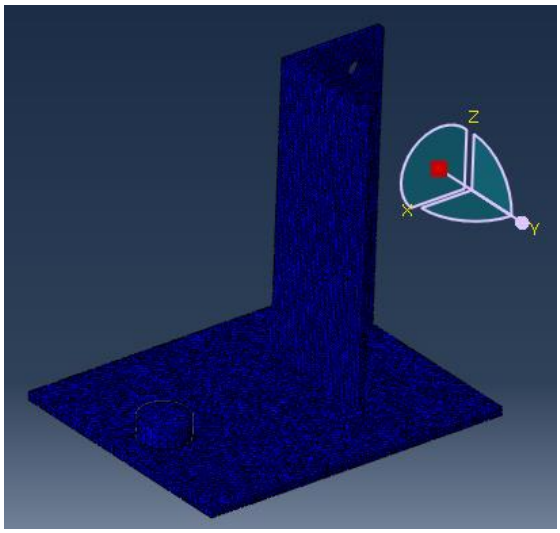

(a)

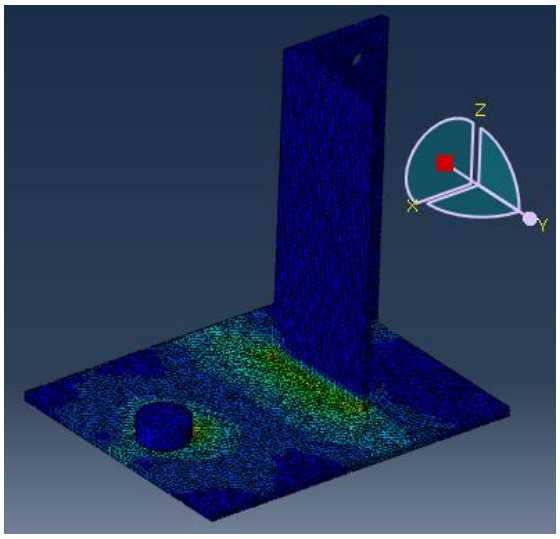

(b)

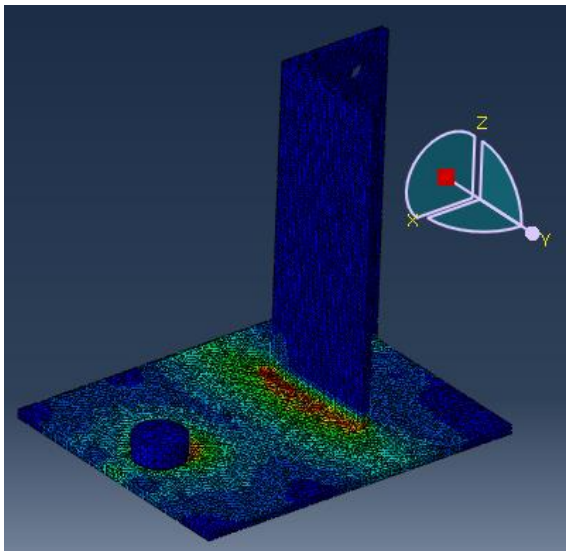

(c)

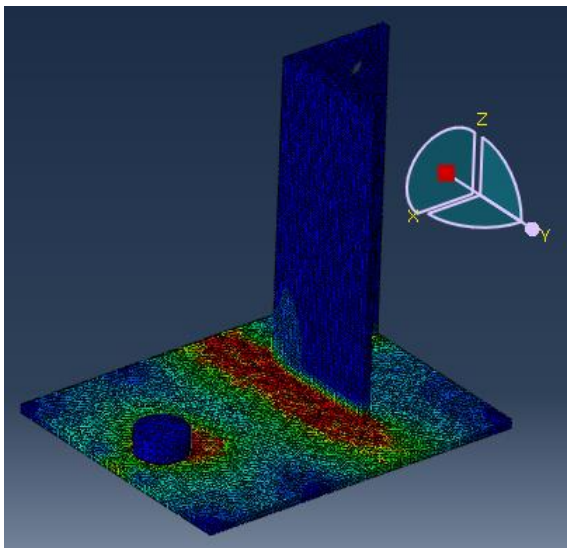

(d)

(Figure 26 (a), (b), (c) and (d))

4.0 Conclusion

The main objective of this thesis focus the validation of the base plate model to a real final values. Of course, the study here presented demonstrates only the uplift tests, so by the end, other studies and this same model with the same nature of displacement control, can be used.

Another point here mentioned is the importance of the segregation of FEA for a macro analysis complementing the CAE modelling and in the end obtaining the desired result.

The conclusions here taken were based on the comparison of the force displacement curves and the resultant deformation shape. The specimen and the CAE model reached the range of 60kN (Figure 27) as well as the last cycle previously determined by the amplitude set. An interesting point to mention is the laboratory presenting an ultimate force in the last cycle as slightly greater than the modelling. Proving itself totally valid as soon as it is predicted that fallowing the same parameters for the bolt, slip contact, friction faces, and the validated material with the fracture rate definition.

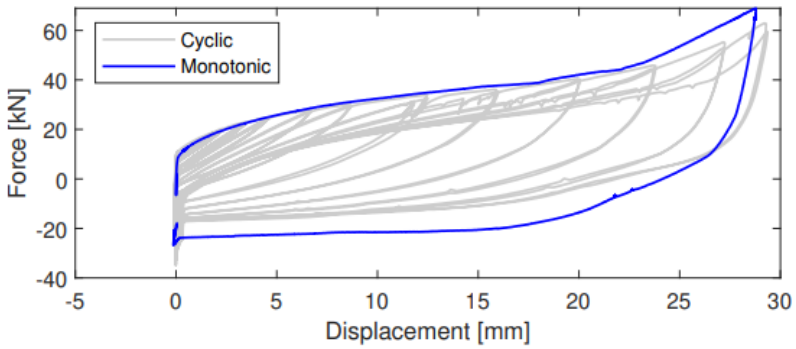

Figure 27: Force Displacement resultant of the specimen of the laboratory

The method implemented here can be used for every matter of comparison with any empirical model on its cyclic uplift on base plates, considering that the mains features here mentioned are preserved in order to be adapted to the FEA and CAE. As well as on preliminary tests for validation of material prior to laboratory trials.

5.0 References

F. A. McClintock, A criterion for ductile fracture by the growth of holes, Journal of Applied Mechanics, vol. 35, no. 2, 1968.

J. R. Rice and D. M. Tracey, “On the ductile enlargement of voids in triaxial stress fields∗,” Journal of the Mechanics and Physics of Solids, vol. 17, no. 3, 1969.

EN 1090-2:2008+A1:2011: Execution of steel structures and aluminium structures — Part 2: Technical requirements for steel structures.

J. W. Hancock and A. C. Mackenzie, “On the mechanisms of ductile failure in high-strength steels subjected to multi-axial stress-states,” Journal of the Mechanics and Physics of Solids, vol. 24, 1976.

Astaneh, A, Bergsma, G., & H, Shen J.,1992. Behavior and Design of Base Plates for Gravity, Wind and Seismic Loads,. National Steel Construction Conference, Las Vegas, Nevada.

EN 16681: 2016 - Steel static storage systems. Adjustable pallet racking systems. Principles for seismic design”.

EN 1993-1-8:2005 + AC:2009, Design of steel structures – Part 1-8: Design of joints.

Myers, A. T., Kanvinde, A. M., Deierlein, G. G., & Fell, B. V. (2009). Effect of weld details on the ductility of steel column baseplate connections. Journal of Constructional Steel Research, 65(6), 1366-1373.

Gomez, Ivan Ricardo, Kanvinde, A., & Deierlein, G. G. (2010). Exposed column base connections subjected to axial compression and flexure. American Institute of Steel Construction.

Ebert, A., Dörre, M., Glienke, R., Behaviour of lockbolts in slip-resistant connections for steel structures, Steel Construction 10 (2017), Issue 4

Crisfield M. A. 2000 Non-linear Finite Element Analysis of Solids and Structures ISBN 0471-92956-5

Stranghöner, N., Afzali, N., Berg, J., Schiborr, M., Bijlaard, F., Gresnigt, N., de Vries, P., Glienke, R., Ebert, A., Influence of different testing criteria on the slip factor of slip-resistant connections, Proceedings of the 13th Nordic Steel Construction Conference, Tampere, Finland, 2015

Ruopp, J.; Kuhlmann, U. (2017): Steel-to-Concrete joints with large anchor plates under shear loading. Steel Construction, 2017, 10, pp. 115-124, DOI: 10.1002/stco.201710015

J.R. Maguire, L.H. Teh, C.L. Lee, G.C. Clifton, J.P.B. Lim, Three-dimensional simulation of the dynamic rocking response of a cold-formed steel pallet rack, in: 2018 NZSEE Conference Papers, 2018.

AISC (1997b), Seismic Provisions for Structural Steel Buildings, April 15, American Institute of Steel Construction, Inc., Chicago, IL.

AISC (2000b), Seismic Provisions for Structural Steel Buildings, Supplement No.2, November 10, American Institute of Steel Construction, Inc., Chicago, IL.

Sulyok Adrian (2019). Fotografii Indrustiale [Photograph]. Retrieved from https://unsplash.com/photos/fgInNyYt2A8 and https://www.sulyokimaging.ro